Targeting the Immune Complex–Bound Complement C3d Ligand as a Novel Therapy for Lupus

Liudmila Kulik,* Jennifer Laskowski,† Brandon Renner,† Rachel Woolaver,† Lian Zhang,‡ Taras Lyubchenko,* Zhiying You,† Joshua M. Thurman,† and V. Michael Holers*

Humoral autoimmunity is central to the development of systemic lupus erythematosus (SLE). Complement receptor type 2 (CR2)/CD21 plays a key role in the development of high-affinity Abs and long-lasting memory to foreign Ags. When CR2 is bound by its primary C3 activation fragment–derived ligand, designated C3d, it coassociates with CD19 on B cells to amplify BCR signaling. C3d and CR2 also mediate immune complex binding to follicular dendritic cells. As the development of SLE involves subversion of normal B cell tolerance checkpoints, one might expect that CR2 ligation by C3d-bound immune complexes would promote development of SLE. However, prior studies in murine models of SLE using gene-targeted *Cr2*$^{-/-}$ mice, which lack both CR2 and complement receptor 1 (CR1), have demonstrated contradictory results. As a new approach, we developed a highly specific mouse anti-mouse C3d mAb that blocks its interaction with CR2. With this novel tool, we show that disruption of the critical C3d–CR2 ligand-receptor binding step alone substantially ameliorates autoimmunity and renal disease in the MRL/*lpr* model of SLE. ***The Journal of Immunology*****, 2019, 203: 3136–3147.**

Systemic lupus erythematosus (SLE) is a chronic autoimmune inflammatory disease that results in widespread damage to multiple organs, including skin, kidney, heart, lungs, and joints (1). The disease course is characterized by the development of autoantibodies directed to nuclear Ags, including DNA, RNA, and histones, as well as other self-proteins. Of particular importance is the generation of self-antigen–containing immune complexes (ICs) and their deposition or local formation in organs, leading to Fc receptor engagement and complement cascade activation, both of which induce intense local proinflammatory processes (1–3). To ameliorate these effects, a major focus of therapeutic development in SLE is to diminish the generation of pathogenic autoantibodies (4, 5).

An important site of IC deposition in patients with lupus and murine models of this disease is the kidney, where IC formation and deposition induce renal inflammation and progressive loss of function, a major cause of morbidity and mortality (4, 6). ICs deposit in the mesangium and in the glomerular capillary wall (subendothelial and/or subepithelial). There, the ICs can directly injure target cells, engage Fc receptors, and activate complement. Once complement is activated within the glomerulus, the membrane attack complex can directly injure nearby glomerular cells, and anaphylatoxins promote infiltration of the glomeruli by leukocytes (7, 8).

Complement proteins play a dual role in lupus development (9). For example, after IC deposition, the C1q protein can initiate complement-mediated inflammation through the classical pathway; however, at the same time, the deficiency of C1q or the lack of C1r, C1s, C2, and C4 predispose to the development of SLE, in part, because of impaired clearance of apoptotic cells (10, 11). Findings observed in humans have been explored by using mice deficient in C1q or C4, in which gene targeting and inactivation of these classical pathway proteins increased lupus risk and caused increased disease severity (9, 12–15). In contrast, the alternative complement activation pathway plays an important role in injury of the kidney and other tissues in lupus models. MRL/*lpr* mice deficient in either of the two essential alternative pathway proteins factor B (fB) or factor D (fD), for example, are protected from renal disease (1, 2, 16, 17).

The C3 protein, synthesized by liver and parenchymal cells, including those in the kidney, is the most abundant complement protein in the blood. It is a key required protein for all three complement activation pathways: classical, alternative, and lectin. Cleavage fragments from C3 generated during complement activation participate in anaphylaxis, target opsonization, IC removal, and humoral B and T cell responses (10, 17–21). The deposition of C3 fragments in the kidney is a key pathologic finding in lupus nephritis. However, with regard to its role in disease, MRL/*lpr* mice deficient in C3 demonstrate greater levels of proteinuria and higher levels of renal IgG deposition rather than protection from a disease similar to fB deficiency (22). In contrast, MASP-1/3–deficient MRL/*lpr* mice, defective in the lectin and alternative complement activation pathways, are protected from glomerulonephritis, but still manifest anti-dsDNA Abs (23).

*Division of Rheumatology, University of Colorado Anschutz Medical Campus, Aurora, CO 80045; †Division of Renal Diseases and Hypertension, University of Colorado Anschutz Medical Campus, Aurora, CO 80045; and ‡Department of Pathology, University of Colorado Anschutz Medical Campus, Aurora, CO 80045

ORCIDs: 0000-0003-2371-4666 (L.K.); 0000-0001-5069-3982 (J.L.); 0000-0002-6060-4119 (B.R.); 0000-0003-1960-2717 (R.W.); 0000-0003-0630-5713 (L.Z.); 0000-0002-3476-9956 (J.M.T.).

Received for publication May 30, 2019. Accepted for publication October 21, 2019.

This work was supported by grants (to V.M.H.) from the Lupus Research Institute (now Lupus Research Alliance) and the National Institutes of Health (R21 AI105717).

Address correspondence and reprint requests to Dr. Liudmila Kulik, Division of Rheumatology, University of Colorado Anschutz Medical Campus, 1775 Aurora Court, 3201L, Aurora, CO 80045. E-mail address: liudmila.kulik@cuanschutz.edu

Abbreviations used in this article: AP, alkaline phosphatase; BUN, blood urea nitrogen; CR, complement receptor; fB, factor B; GC, germinal center; IC, immune complex; ID, identifier; MZ, marginal zone; PAS, periodic acid–Schiff; PBS-T, PBS containing 0.05% Tween 20; qPCR, quantitative PCR; RT, room temperature; R.U., relative unit; SLE, systemic lupus erythematosus.

Once C3 is cleaved to C3b, the transiently exposed thioester bond participates in a transacylation reaction with nucleophilic groups present on cell surfaces, complex carbohydrates, or ICs (22). C3b can complex with C4b2b (C3 convertase) to form a C5 convertase, leading to membrane attack complex formation. It can also bind to fB, forming the alternative pathway C3 convertase and initiating new C3 cleavage (referred to as the amplification loop). Bound C3b can also be inactivated to the iC3b protein form by factor I in concert with certain complement regulatory proteins acting as cofactors (24). iC3b is subsequently converted to C3dg by factor I and complement receptor (CR) 1 and then to C3d by proteases. During C3 fragment cleavage, iC3b is a ligand for CR2. C3d and C3dg are also ligands for CR2, which itself is a coreceptor in the B cell activation pathway.

The interaction of Ag-bound C3d with CR2, in association with CD19, is required for memory cell development and affinity maturation of Abs (25–28). Mice, in contrast to humans, have alternative splicing of the same *Cr2* gene coding for both CR1 and CR2 proteins; therefore, targeted mutation of the *Cr2* gene prevents the production of both proteins. $Cr2^{-/-}$ mice on a B6 background are not predisposed to autoantibody production, and humans deficient in CR2 develop hypogammaglobulinemia but not autoimmunity (29). When the *Cr2*-deficient genotype was bred onto the B6/*lpr* background, however, the mice developed increased titers of antinuclear and anti-dsDNA Abs and lymphadenopathy but not proteinuria or changes in spleen size, suggesting that the CR2/CR1 interaction was required for tolerance to nuclear autoantigens (30). In another lupus-related study, although loss of CR2 and CR1 or inhibition of CR2 on follicular dendritic cells led to decreased IFN-α generation, the mice developed milder neurologic alterations than control mice (31). Similarly, it was shown that the soluble C3d ligand binding the CR2 protein domain, either alone or tagged with complement inhibitors, was able to reduce disease features in two lupus-prone mice strains, (NZBxNZW)F_1 and MRL/*lpr* mice (11, 32). Thus, the effects of modulating the complement system in lupus vary by pathway, receptor, and specific protein modulated and disease context, and they reflect the complex roles of the system in modulating the innate–adaptive immune interface as well as generating potent effector mechanisms.

MRL/*lpr* mice spontaneously develop a severe autoimmune syndrome resembling human SLE. The MRL/*lpr* strain has high concentrations of circulating Igs, which include elevated levels of autoantibodies, such as anti-nuclear Abs, anti-ssDNA, anti-dsDNA, anti-Sm, and rheumatoid factors, resulting in large amounts of ICs. MRL/*lpr* mice spontaneously develop progressive lymphadenopathy, hypergammaglobulinemia, autoantibody production, and IC formation, leading to vasculitis, arthritis, and fatal renal failure (33, 34).

Recently we developed a set of new mAbs to the human and mouse C3d protein (35). A subset of mAbs were capable of blocking the binding of the C3d ligand to CR2 in an ELISA. We hypothesized that blockade of the CR2–C3d interaction in vivo by targeting C3d itself could dampen the immune response to C3d-opsonized Ags, and also attenuate disease severity in models of SLE. To test this hypotheses, we treated mice with mAb 3d-8b, initially before inducing immunity to a T cell–dependent Ag and then to examine the effects of mAb 3d-8b in the MRL/*lpr* model of lupus.

Materials and Methods

Mice

All mice were maintained in specific pathogen–free facilities at the University of Colorado Anschutz Medical Campus. Animal procedures were approved by the Institutional Animal Care and Use Committee. Wild-type B6 (stock number: 000664) mice from The Jackson Laboratory were bred in the local animal facility, and females age 6–8 wk were used in experiments for mAb effects on SRBC immunization, Ca^{2+} influx, germinal center (GC) formation, and circulatory pharmacokinetics. C3-deficient ($C3^{-/-}$) mice on the B6 background were bred in the local animal facility. Lupus-prone female MRL/*lpr* mice (stock number: 000485) were also purchased from The Jackson Laboratory and maintained in the local animal facility until achieving the correct age for experiments.

SRBC immunization

SRBC (Colorado Serum, Denver, CO) were washed three times with PBS and diluted to working concentrations. Mice were injected i.p. with 200 μl of 1×10^7 SRBC per mouse. Detection of Ab to SRBC was measured by ELISA, as described previously (36, 37). Bound Abs were detected by incubation with alkaline phosphatase (AP)–conjugated anti-mouse IgG1 Ab (Jackson ImmunoResearch), followed by washing and addition of *p*-nitrophenyl phosphate as the AP substrate (Sigma-Aldrich) at a concentration 1 mg/ml. To calculate relative units (R.U.), the mean OD at 405 nm from triplicate wells was compared with a standard curve of OD measurements of serially diluted pooled high-titer anti-SRBC serum.

Ca^{2+} influx

Ca^{2+} influx was performed as previously described (38). Briefly, isolated mouse splenocytes were Indo 1-AM loaded (5 μM for 30 min at 37°C) and stained with CD45R/B220–FITC Ab (BD Pharmingen). Cells were stimulated with premixed complexes containing 0.01 μg/1 $\times$ 10^6 cells/ml biotinylated $F(ab)'_2$ goat anti-mouse IgM, C3dg-biotin (2 μg/ml) and streptavidin (ST; 0.001 μg/ml). $Ca2^+$ flux was measured in gated $B220^+$ cells. To determine whether mAb 3d-8b binding to C3dg blocks CR2 engagement by the ligand, mAb 3d-8b was added to the anti-IgM/C3dg-biotin in a concentration 5 μg/ml before the induction of Ca^{2+} influx. Experiments were performed at room temperature (RT) on a BD LSR flow cytometer (BD Biosciences), and intracellular Ca^{2+} influx was analyzed using FlowJo software.

*Treatment of MRL/*lpr *mice with anti-C3d mAb 3d-8b*

Female MRL/*lpr* mice were randomly divided into three groups and injected at week 13 or 14 with 300 μl of PBS containing 2 mg/mouse with either mAb 3d-8b (first group), 2 mg/mouse isotype control IgG (second group), or 300 μl of PBS as a vehicle control (third group). Blood and urine samples were collected every other week. At week 22, mice were bled by cardiac puncture, the kidneys were removed, and the mice were sacrificed. One kidney from each animal was fixed with 10% buffered formalin. Fixed kidneys were embedded in paraffin and then sectioned before staining with periodic acid–Schiff (PAS) to quantitatively evaluate injury. The other kidney was cut in half sagittal. One half was embedded in OCT medium, snap frozen, and stored at −80°C for fluorescence microscopy. The other kidney half was snap frozen and stored at −80°C for RNA isolation and RT-PCR mRNA quantitation.

Anti-dsDNA Ab ELISA

Anti-dsDNA Ab levels were measured by ELISA, as previously described (39). Briefly, Immulon-2B plates (Thermo Fisher Scientific) were coated with 5 μg/ml double-stranded calf thymus DNA (Sigma-Aldrich) in sodium salt citrate buffer at RT overnight. After washing with PBS containing 0.05% Tween 20 (PBS-T), plasma samples were added in serial dilutions starting at 1/100 and incubated for 2 h at RT. After washing with PBS-T, AP-conjugated goat anti-mouse IgG Ab (γ-chain specific) (Jackson ImmunoResearch) were added for 1 h. Plates were washed with PBS-T and substrate *p*-nitrophenyl phosphate (Sigma-Aldrich) at 1 mg/ml was added. Plates were read at 405 nm. To calculate R.U., the mean OD at 405 nm from triplicate wells was compared with a standard curve of OD measurements of titrated standard high-titer serum.

Urine albumin and blood urea nitrogen measurement

Urine albumin was measured by an ELISA, according to the manufacturer's instructions (Bethyl Laboratories, Montgomery, TX). Urine creatinine was measured using an Alfa Wasserman ACE Chemistry Analyzer. Creatinine was used to normalize urine albumin excretion. Blood urea nitrogen (BUN) was measured using an Alfa Wasserman ACE Chemistry Analyzer.

Flow cytometry

Spleen cells were dissociated between frosted glass slides, and splenocytes were isolated. RBC were removed by ACK lysis buffer (0.15 M NH_4Cl, 1 mM $KHCO_3$, 0.1 mM NaEDTA [pH 7.2–7.4]). After RBC lysis by ACK buffer, nucleated cells were washed by spinning and then resuspended in staining buffer (2% BSA/0.02% NaN_3/PBS) at a concentration of 1×10^7/ml. Ten microgram per milliliter 2.4G2 mAb to block FcγR were added to

cells for 15 min and incubated on ice, following which cells were washed in staining buffer and resuspended $1 \times 10^6/100$ μl staining buffer containing biotinylated or fluorochrome-labeled Abs to specific cell surface markers. Abs used in the experiments included anti-CD45R/B220, GL-7, anti-CD4, anti-CD8, anti-mouse CD21 (7G6), and anti-CD19 from BD Biosciences. Anti-mouse CD35 (8C12) and anti-mouse CR1/CR2 (4B2) were purified and biotinylated in the laboratory. Cells were incubated for 30 min on ice in the dark. After incubation, cells were washed in staining buffer two times and then incubated with the appropriate ST-conjugated fluorochrome to detect biotin-labeled mAb. Following incubation, cells were washed as above and then resuspended in PBS containing 1% formaldehyde. Flow cytometry was carried out using a Gallios flow cytometer.

Fluorescence microscopy

Frozen sections (6 μm thick) from a subset of mice were stained as described with FITC anti-mouse C3 (MP Biomedicals), Cy3–anti-mouse IgGγ (Jackson ImmunoResearch), Cy3 anti-mouse IgM (μ-chain specific) (Jackson ImmunoResearch), and Alexa Fluor 488 anti-mouse IgGγ (Invitrogen). An Olympus FV1000 FCS/RICS confocal microscope and Olympus FV10-ASW software were used for image acquisition, conversion, and intensity analysis. For that, 20–25 glomeruli of each kidney were randomly chosen and analyzed blindly for intensity of the red and green dyes, and intensity is presented as relative fluorescence units for each glomerulus. An independent blind analysis was performed on PAS-stained sections for glomeruli of each kidney. Fifty glomeruli were randomly chosen from each kidney and were analyzed for mesangial and endocapillary hypercellularity as well as for crescent formation and necrosis.

Quantitative RT-PCR

Kidney RNA isolation was performed by the TRIzol method combined with column purification. For that, one half of snap-frozen kidney was ground with a pestle in an Eppendorf tube with 1 ml of TRIzol. The supernatant was transferred into a new tube and incubated for 5 min. One hundred microliters of chloroform was added, and the tube was shaken and left standing for 2 min. Tubes were spun for 15 min at 4°C, and the upper phase (300 μl) was transferred into new tube. Three hundred microliters of 70% ethanol was added, and the tube was mixed and transferred to the RNeasy Plus Universal Mini Kit spin columns (QIAGEN). Columns were spun, and 700 μl of commercial RWT buffer (QIAGEN) was added to the wash columns. After centrifugation, columns were washed twice with 500 μl of commercial RPE buffer (QIAGEN). Elution was performed using 30 μl RNase-free water. Purity and quality of RNA was confirmed using 1.5% formaldehyde/agarose gel. High-quality RNA was reverse transcribed using random primers and SuperScript II. Bio-Rad Laboratories' commercial primers with unique assay identifier (ID) number for Ccl2 (ID: qMmuCED0048300), Ccl3 (MIP1) (ID: qmMuCED0003870), Il-10 (ID: qmMuCED0044967), Il-6 (ID: qmMuCID0005613), Tnf (ID: qmMuCED0004141), Tnfst13 (APRIL) (ID: qmMuCED0003844), Tgfb1 (ID: qmMuCID0017320), Ccl5 (ID: qmMuCID0021047), 11b (ID: qmMuCED0045755), Pdgfb (ID: qmMuCID0017307), and Ppia (ID: qmMuCED0041303) were used. PCR was performed on a Genetic Analyzer (Applied Biosystems/Hitachi). For the internal reference genes, peptidylprolyl isomerase A (Ppia), ribosomal protein L37 (Rpl37), and actin were chosen. The PCR was performed on a Light Cycler 480 II (Roche). ΔCq, the difference between cycle threshold (Cq) of the sample and Cq of the reference gene, was used to calculate total RNA abundance.

Circulating IC ELISA

Circulating IC levels were determined by the C1q ELISA method, as previously described (22). ELISA plates were coated with 10 μg/ml human C1q (Sigma-Aldrich) in 0.1 M carbonate buffer (pH 9.6), incubated for 48 h at 4°C, blocked for 2 h at RT with 1% BSA in PBS, and washed with PBS. EDTA-treated plasma samples were added in serial dilutions starting at a 1:50 dilution, and plates were incubated for 1 h at RT and overnight at 4°C. The assay was then performed, as described above, with HRP-conjugated goat anti-mouse IgG (γ-chain specific) (Jackson ImmunoResearch).

Results

mAb 3d-8b interferes with CR1/CR2 binding of iC3b/C3d and impairs immunological responses to T-dependent Ags

The humoral immune response to SRBC has previously been shown to be dependent upon both C3 and CR1/CR2 expression (40). To evaluate the effects of treatment with mAb 3d-8b on the immune response to T-dependent Ags, wild-type B6 mice were injected i.p. with 1.5 mg of mAb 3d-8b 1 d before immunization with SRBC. Control mice were injected with mAb 3d-11, an anti-C3d mAb that does not block binding of C3d to CR2 (35). As shown in Fig. 1A, treatment with mAb 3d-8b decreased anti-SRBC IgG1 Ab levels, as analyzed at day 17 after SRBC immunization. Notably, development of IgM anti-SRBC was not affected by mAb 3d-8b injection. Similar results were obtained 30 d after the first immunization (data not shown) and also for the secondary response after immunization with the same amount of SRBC at day 34, followed by analysis at day 10 (Fig. 1B). Similar to the primary immunization experiment, a marked reduction in anti-SRBC Ab level after second immunization with SRBC was seen in mice previously injected with mAb 3d-8b (Fig. 1B). No reduction in anti-SRBC IgG1 was observed in control mice injected with mAb 3d-11. Some reduction, however, not statistically significant, was seen for IgM in mice injected with mAb 3d-8b.

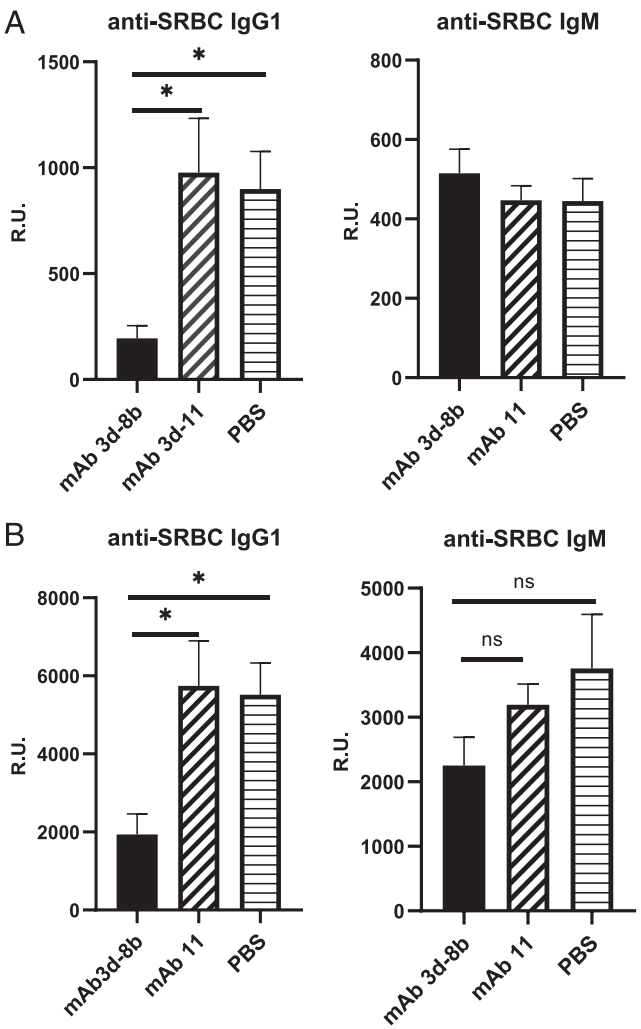

FIGURE 1. mAb 3d-8b is able to block CR2/C3d interaction in vivo and diminish a T-dependent immune response. (**A**) Thirty wild-type B6 mice were split into three groups and preinjected with 1.5 mg/mouse mAb 3d-8b (10 mice), nonblocking CR2/C3d mAb 3d-11 (10 mice), or PBS (10 mice). Eighteen hours later, mice in each group were immunized i.p. with the T-dependent Ag SRBC at 1×10^7 SRBC per mouse. Ab production to SRBC, both IgM and IgG1, was analyzed on day 17. In (**B**), the same mice were boosted later with the same amount of SRBC on day 34, and blood samples were taken 10 d later for the ELISA analysis. Bars represent average (mean) R.U. data calculated for all 10 mice of one particular group. Error bars represent SD. Data are representative of two independent experiments. Statistical analyses were performed by one-way ANOVA. *$p < 0.05$. ns, not statistically significant.

To support that the reduced immunologic response observed in mice injected with mAb 3d-8b was caused by interference with the CR2 costimulatory signal for the BCR, we next determined whether blocking the CR2/C3d signal would reduce CR2/CD19–amplified calcium signaling by B cells in vitro. As has been reported previously, a CR2-dependent Ca^{2+} influx signal can be triggered in B cells by treating the cells with complex anti–IgM-b/C3dg-b/ST consisting of ST cross-linked biotinylated C3dg combined with a suboptimal dose of biotinylated anti-BCR (41). As shown in Fig. 2A, neither stimulation with a suboptimal dose of anti-BCR (dotted gray line) nor C3dg-biotin (data not shown) alone demonstrated a detectable increase in the level of intracellular Ca^{2+}. However, when anti–IgM-b/C3dg-b/ST complex was added to splenocytes, a robust Ca^{2+} influx was seen in $B220^+$ splenic B cells, which was similar to one when the anti–IgM-b/C3dg-b/ST complex was preincubated for 120 s with 5 μg/ml isotype control (thick black line). When the anti–IgM-b/C3dg-b/ST complex was preincubated with 5 μg/ml mAb 3d-8b, a complete abrogation in Ca^{2+} influx was seen (thin black line), confirming that mAb 3d-8b binds C3dg with sufficiently high affinity and blocks C3dg from binding to CR2 and amplifying the Ca^{2+} influx.

To further delineate the effects of mAb 3d-8b on B cell activation in vivo, we analyzed GC formation in mice injected with isotype control or mAb 3d-8b and immunized with SRBC. We found that spleens from mice preinjected with mAb 3d-8b developed lower numbers of $GL7^+$ cells, which reflect GC formation, and lower numbers of $CD138^+B220^{lo}$ plasma cells and trend toward a reduction of $CD138^+$ $B220^+$ plasmablasts in mAb 3d-8b–injected mice (Fig. 2B), confirming that mAb 3d-8b injection has an inhibitory effect on Ag-specific B cell responses in vivo.

As shown previously (35), mAb 3d-8b does not bind intact C3 but binds to C3 breakdown products iC3b, C3dg, and C3d found in tissues. To measure the pharmacokinetics of mAb 3d-8b and to determine whether it was affected by binding to endogenous C3 fragments, we measured the $t_{1/2}$ of mAb in C3-sufficient as compared with $C3^{-/-}$ mice. We injected wild-type B6 mice and B6 $C3^{-/-}$ mice with either isotype control mAb (recognizing OVA) or mAb 3d-8b. Mice were bled 1, 9, and 18 d later, and the level of both 3d-8b and control mAb in serum was analyzed by ELISA. As shown in Fig. 3, wild-type B6 mice demonstrated a substantially faster clearance of mAb 3d-8b from blood as compared with $C3^{-/-}$ mice. We were able to detect 2 μg/ml mAb 3d-8b at day 18 in B6 mice, a level that was in 75 times lower than the amount of 3d-8b Ab in $C3^{-/-}$ mice. The level of mAb 3d-8b that we were able to measure in this ELISA was 0.01 ng/ml.

*A single injection of anti-C3d mAb 3d-8b reduces anti-dsDNA autoantibody production and partially ameliorates proteinuria in MRL/*lpr *mice*

To determine the effects of mAb 3d-8b on the development of lupus-like disease, we injected 13-wk-old MRL/*lpr* mice with 2 mg of mAb 3d-8b, isotype control mAb, or PBS buffer alone. Mice were bled every other week, and plasma samples were assayed for anti-dsDNA Ab. As shown in Fig. 4A, mice injected with mAb 3d-8b demonstrated a substantially decreased level of anti-dsDNA IgG within 4 wk of the injection, and this effect was still evident after 8 wk.

In addition, urine samples were collected, and albuminuria was analyzed by ELISA (Fig. 4B). The level of urine creatinine was used to standardize the albumin concentration. The level of albuminuria was reduced in mice treated with mAb 3d-8b compared with control animals at 4 and 8 wk but not 6 wk after injection. This result suggests that treatment with mAb 3d-8b partially protected the mice from the development of kidney damage.

To evaluate the effects of treatment with mAb 3d-8b on additional biomarkers of relevance to this disease process, we injected 14-wk-old MRL/*lpr* mice with 2 mg of mAb 3d-8b, isotype control mAb, or PBS buffer alone (Fig. 5A). Mice were then followed until they reached 22 wk of age. Urine samples were taken every other week and the day before sacrifice. Similar to what was observed in the previous experiment, a trend in reduction of albuminuria was seen 8 wk following injection (Fig. 5A). BUN levels also trended lower in mice treated with mAb 3d-8b compared with control mice, further suggesting that treatment with mAb 3d-8b provided an ameliorative effect on kidney injury. We again observed a substantial reduction in anti-dsDNA Ab titers in the group treated with mAb 3d-8b (Fig. 5A).

Importantly, we found that mAb 3d-8b injection did not affect the blood level of circulating IC, as we found similar levels of ICs in plasma taken from these three groups of mice 8 wk after injection (Fig. 5B). In contrast, we found that the level of total IgG to be higher in the mAb 3d-8b–injected group.

C3 fragment and IgG deposition and level of kidney injury in mice injected with mAb 3d-8b

We next examined the kidneys of mice injected either with isotype control or mAb 3d-8b as well as vehicle (PBS)-injected mice. Fluorescence microscopy showed a nonsignificant trend in reduction of C3 deposition in glomeruli of mice treated with mAb 3d-8b compared with control IgG–injected mice. A similar nonsignificant trend in reduction of C3 deposition was seen to mAb 3d-8b–injected mice as compared with PBS-injected mice (Fig. 6A). The IgG deposition in glomeruli of mAb 3d-8b–injected mice also showed a reduction but was not statistically significant. Although glomeruli in 3d-8b–treated mice still showed inflammatory changes, crescents (a sign of severe glomerular injury) and necrosis were not seen in any of the mAb 3d-8b–treated mice (Fig. 6B).

Reduced level of a subset of proinflammatory cytokines and chemokines in kidneys of mice injected with mAb 3d-8b

As another measure of efficacy, quantitative PCR (qPCR) for known chemokines upregulated in inflamed tissue or chemokines involved in inflammation reduction (42) was performed. IL-10, IL-1b, IL-6, TGF-b, APRIL, MIP-1, CCL2, and CCL-5 mRNA levels were measured in kidneys from mice that received mAb 3d-8b, control mAb, or PBS treatment. The data are shown as relative RNA abundance for the particular mRNA expressed in the three groups of mice. Fig. 7 demonstrates the fold reduction in mRNA level (average) for a particular transcript expressed either in mAb 3d-8b–injected or control mAb–injected mice. We identified three genes with markedly decreased levels of mRNA in kidneys of mice treated with mAb 3d-8b. The downregulation in mRNA observed for the proinflammatory IL-6 chemokine is consistent with the reduced inflammation in 3d-8b mAb–injected mouse kidneys. Two more chemokines, CCL2 and CCL5 (RANTES), also demonstrate reduced level of RNA in kidneys from mAb 3d-8b–injected mice. Both chemokines recruit leukocytes into sites of inflammation; for example, CCL2 recruits monocytes, memory T cells, and dendritic cells, whereas CCL5 is chemotactic for T cells, eosinophils, and basophils. Reduction in these two chemokines is consistent with a lower level of inflammation in mAb 3d-8b–injected mice. Some downregulation of CCL-2 and IL-6 mRNA was observed in control IgG–injected mice, although this downregulation was NS if compared with PBS-injected group.

T and B cell populations not affected by mAb 3d-8b

To determine whether mAb 3d-8b injection demonstrates substantial effects on splenic B cells, we injected 7- and 14-wk-old

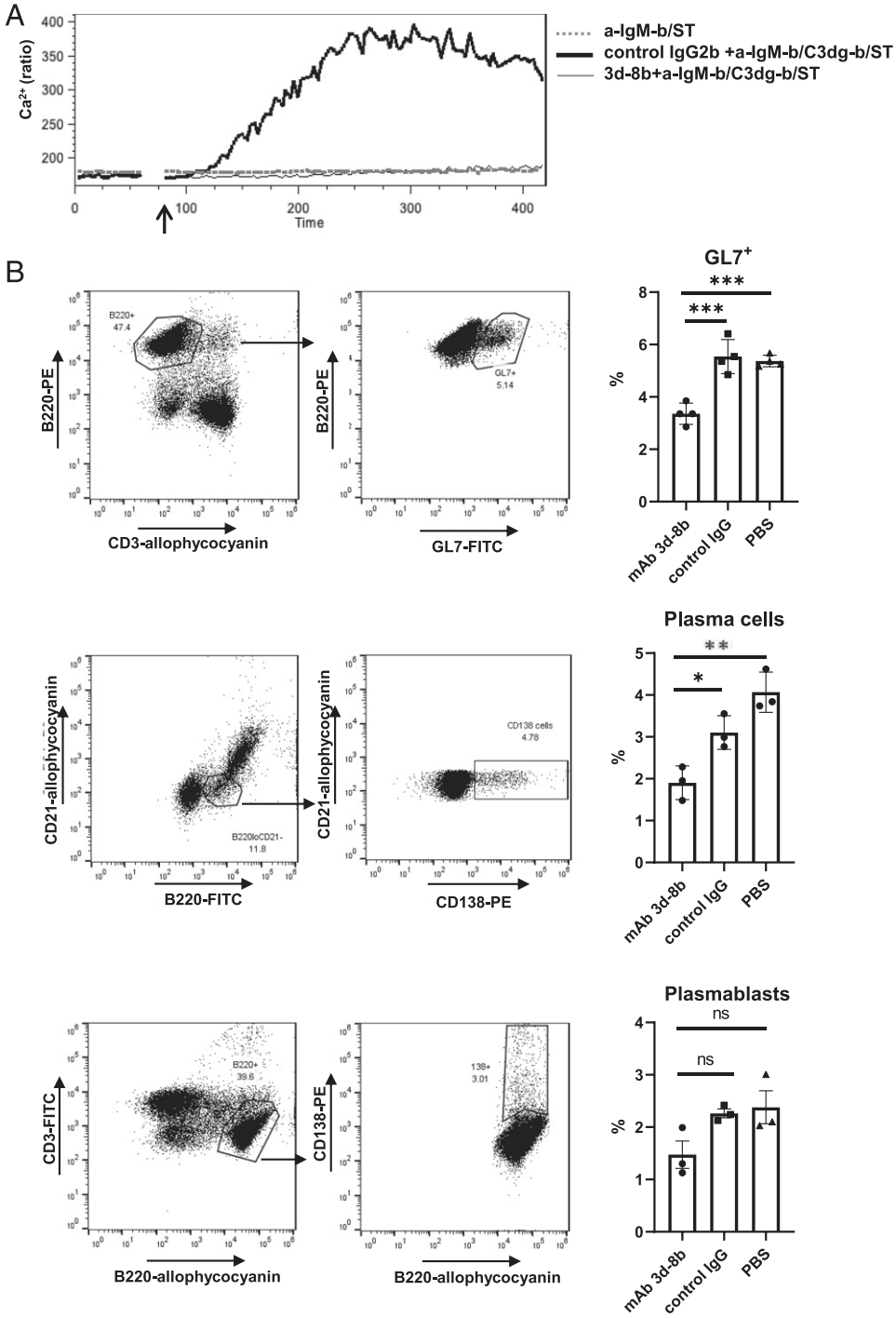

FIGURE 2. Binding of mAb 3d-8b to C3d blocks CR2 engagement and diminishes B cell– activation signaling. (**A**) Erythrocyte-depleted splenocytes from B6 mice were loaded with Indo-1 AM and stained with anti-CD45R(B220)–allophycocyanin Ab. The $B220^+$ cells were gated, and the ability to generate Ca^{2+} influx in response to anti-BCR combined with CR2 ligand (anti–IgM-b/C3dg-b/SA) was analyzed for the $B220^+$ gated cell population. Prior to adding the anti–IgM-b/C3dg-b/SA complex to cells, the complex was preincubated for 2 min with 5 μg/ml mAb 3d-8b to block the CR2 binding site on C3d (thin dark) or isotype control IgG (OVA 11) mAb (thick dark). The suboptimal concentration of anti-IgM Ab alone (anti–IgM-b/SA) was not able to induce Ca^{2+} influx (dotted gray). The arrow shows the timepoint when stimuli were added to the cells. (**B**) Injection of mAb 3d-8b interferes with GC formation and B cell transition to Ab-producing cells. B6 mice, three for each condition, were preinjected with 2 mg of mAb 3d-8b, isotype control IgG2b, or PBS. Eighteen hours later, they were immunized with 1×10^8 SRBC per mouse. Eleven days later, splenocytes were isolated and stained with anti-CD3–allophycocyanin and anti-CD45R(B220)–PE as well as the marker for GC cells, GL7-FITC. $CD3^-/B220^+$ cells were analyzed for the percentage of $GL7^+$ cells on the $B220^+$ cells (upper row). Plasma cells have a low level of B220 expression and are $CR2^-$. To analyze plasma cell development in mice treated in the three conditions as described above, mice splenocytes were analyzed with anti-CR2–allophycocyanin, anti-CD45R(B220)–FITC and anti-CD138–PE Ab. $B220^{lo}$ and CR2-negative cells were gated, and the percentage of $CD138^+$ cells in $B220^{lo}CR2^-$ population was calculated in a new plot for CD21–allophycocyanin and CD138-PE (middle row). In contrast to plasma cells, plasmablasts exhibit B220 marker expression similar to mature B cells. To compare the percentage of plasmablasts we have in B cell population, we stained splenocytes with anti-B220–allophycocyanin and anti-CD3–FITC Ab. Gated $B220^+CD3^-$ cells were reanalyzed for $B220^+CD138^+$ cell percentage in a new plot for B220–allophycocyanin and CD138–PE (bottom row). Bars represent average in percentage for $GL7^+$ cells or plasmablasts and plasma cells in spleens of mice from three different conditions. Error bars represent SD for particular group of data. Statistical analyses were performed comparing data obtained for mAb 3d-8b–injected mice to control Ab– or PBS-injected mice. Statistical analyses were performed by one-way ANOVA. $*p < 0.05$, $**p < 0.01$, $***p < 0.001$. ns, not significant.

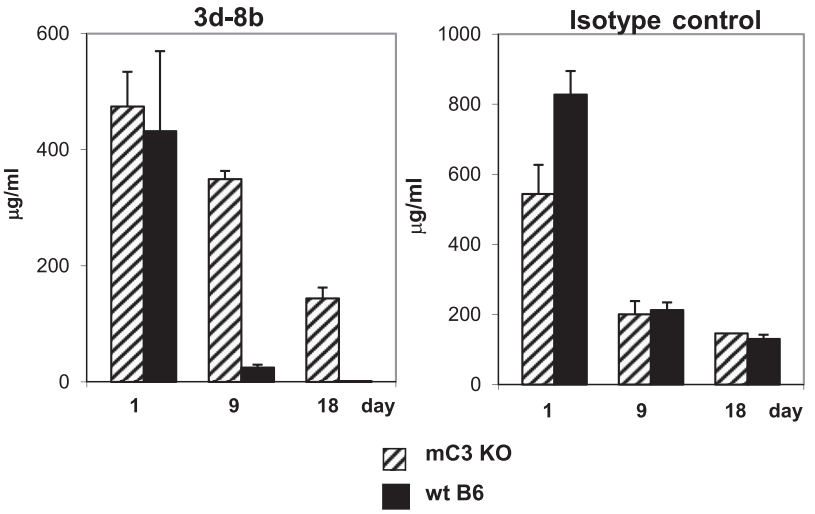

FIGURE 3. The $t_{1/2}$ circulating in blood of mAb 3d-8b is decreased in C3-sufficient animals. $C3^{-/-}$ mice (C3 KO [knockout], $n = 3$) and wild-type (wt) B6 mice ($n = 3$) were injected with 1.5 mg of mAb 3d-8b. Similarly, two groups of mice were injected with isotype control IgG2b (anti-OVA mAb). Mice were bled at 22 h and 9 and 18 d later. The level of mAb 3d-8b was measured in ELISA with recombinant mC3d as the substrate. Control Ab detection was done using an OVA ELISA. The level of mAb 3d-8b did not decrease quickly at early timepoints (22 h); however, with time, the Ab was eliminated to a very low level (2 µg/ml) at day 18. Elimination was C3 dependent, as the C3 KO mice demonstrated different kinetics of mAb 3d-8b reduction in the blood. The kinetics of 3d-8b elimination from C3 KO mice was similar to that observed for isotype control mAb.

MRL/*lpr* mice with either mAb 3d-8b, control mAb, or with PBS vehicle control. The 7-wk-old mice were used as a control for later changes in B and T cell populations induced by the disease development, as these mice do not yet demonstrate the major disease findings seen in older MRL/*lpr* mice. Mice were sacrificed either 24 h after injection or 1 wk later. Isolated splenocytes were stained with CD19–allophycocyanin, CD23–PE, and CD24–FITC to identify follicular

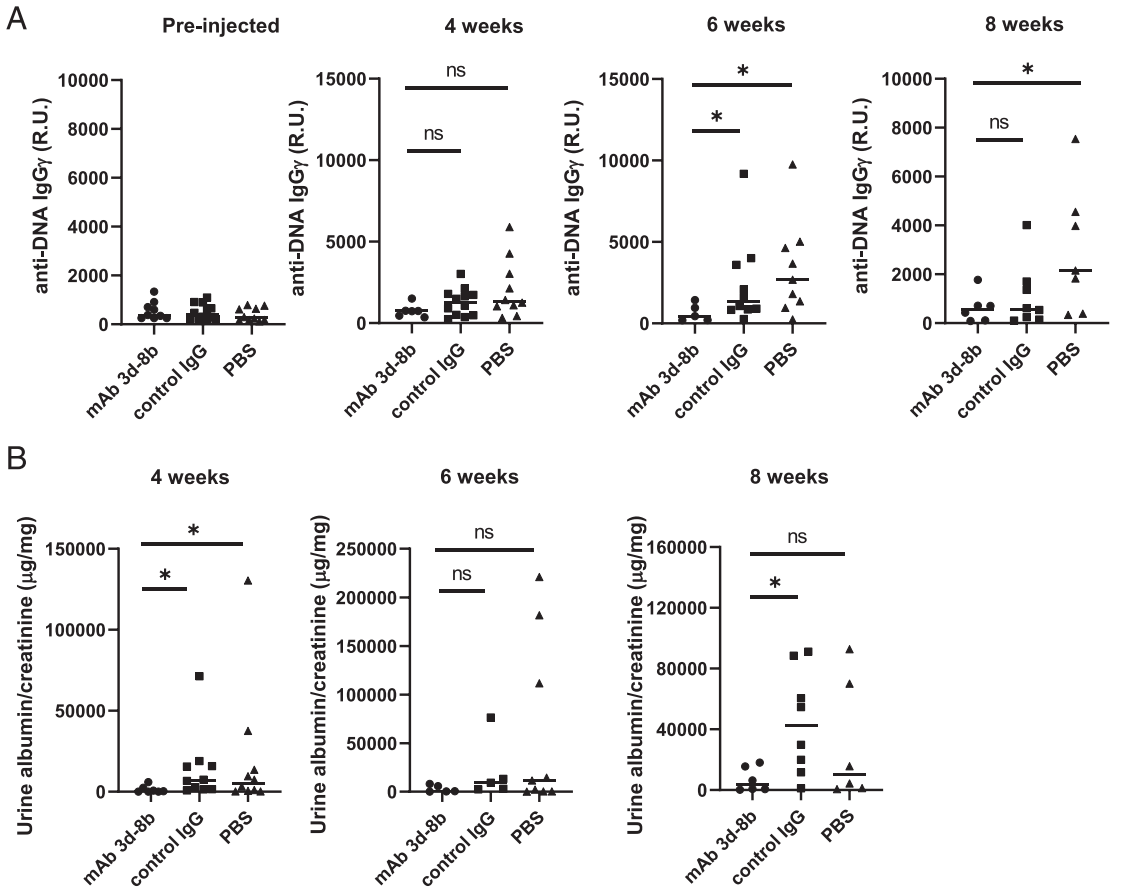

FIGURE 4. Single injection of mAb 3d-8b results in a long-lasting ameliorative effect on autoantibody production and proteinuria. (**A**) Thirteen-week-old MRL/*lpr* mice were divided into three groups with 12 mice in each group and injected with 2 mg/mouse mAb 3d-8b (circle), 2 mg/mouse of isotype control mAb (square), or PBS alone (triangle). Each symbol represents data for an individual mouse. The horizontal line is the average for each group. The level of anti-dsDNA IgG Ab in plasma, presented in R.U., shows that mice injected with mAb 3d-8b demonstrate a dramatic reduction in dsDNA Ab production. (**B**) Urine samples were obtained from the same mice and analyzed for the level of proteinuria. For that, the level of albumin was normalized using the creatine level in the same urine sample. The level of proteinuria was also substantially reduced in mice injected with mAb 3d-8b. Included is a representative experiment from three independent studies. Statistical analysis was performed by one-way ANOVA with adjustment for multiple comparisons using the Dunnett–Hsu test. $*p < 0.05$. ns, not statistically significant.

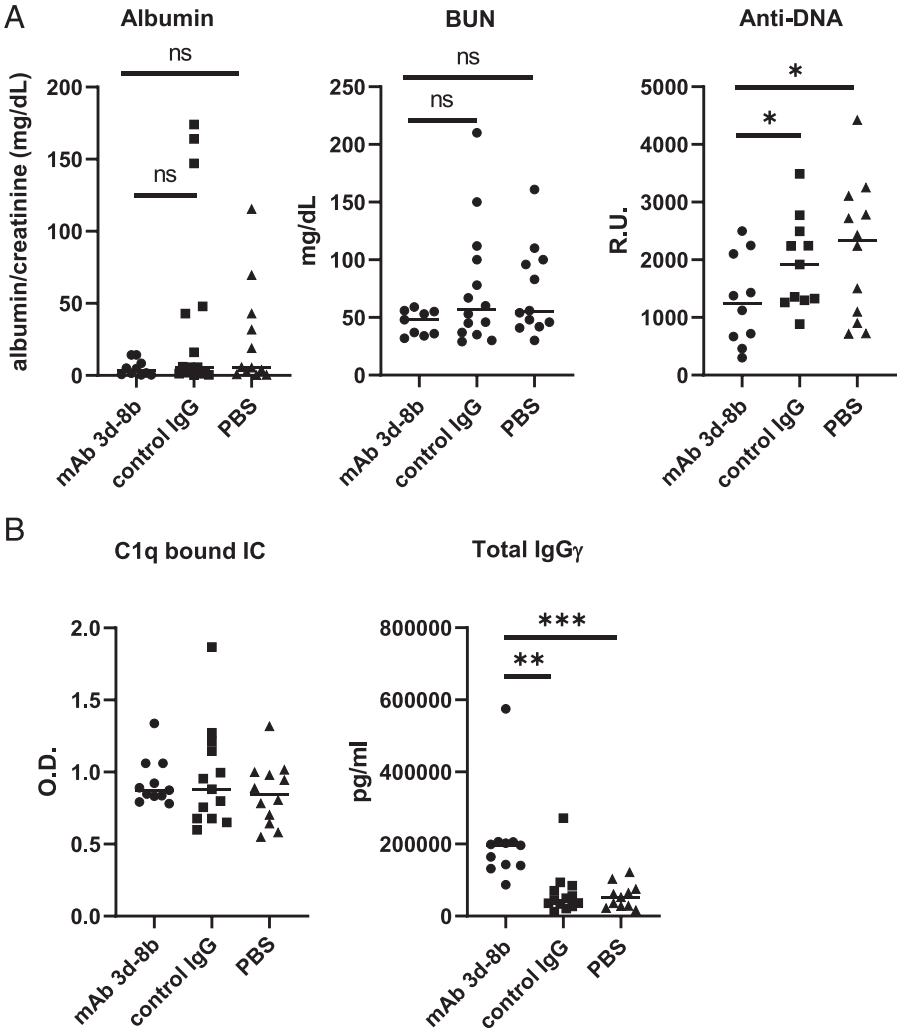

FIGURE 5. Circulating IC and total IgG levels in the blood as compared with Abs and renal function in another cohort. (**A**) Three groups of 14-wk-old MRL/*lpr* mice, 20 for each condition, were injected with 2 mg/mouse of mAb 3d-8b (circle), isotype control Ab (square) or PBS alone (triangle). Eight weeks later, samples of urine were analyzed for the level of excreted mouse albumin to determine the level of proteinuria in the three groups of mice. Once again a trend in reduction in proteinuria was observed in mice injected with mAb 3d-8b. BUN levels also trended in a protective direction and suggested reduced kidney damage in mAb 3d-8b–treated mice. Plasma samples from mice were also analyzed for the level of anti-dsDNA Ab, and again, demonstrated reduced levels in mice injected with mAb 3d-8b. (**B**) Injection of mAb 3d-8b did not affect circulating IC levels. Interestingly, mAb-injected mice, although demonstrating reducing autoantibody production to dsDNA Ag, showed increased total IgG levels. Statistical analyses were performed by one-way ANOVA with adjustment for multiple comparisons using the Dunnett–Hsu test. $*p < 0.05$, $**p < 0.01$, $***p < 0.005$. ns, not statistically significant.

($CD23^+$, $CD24^-$), marginal zone (MZ) ($CD23^-$, $CD24^-$), transitional ($CD23^+$, $CD24^+$), and immature ($CD23^-$, $CD24^+$) B cells. There were no statistically significant changes in B cell subpopulations due to either PBS-, control-, or mAb 3d-8b–injected mice at either at 1 wk (Fig. 8A) or 24 h after injection (data not shown). A trend in MZ cell upregulation and follicular cell downregulation was observed in 14-wk-old mice injected with mAb 3d-8b; however, these changes were not statistically significant. The upregulation in MZ and downregulation in transitional B cells seen in 14-wk-old mice, marked with a star, are due to age related changes in this strain of mice but not mAb 3d-8b injection.

Similarly, no changes in the percentage of CD8, CD4, or CD19 cell populations were detected in either blood (data not shown) or spleens of mice injected with mAb 3d-8b or control (Fig. 8B). The 14-wk-old mice already have a lower percentage of $CD19^+$ cells caused by an emerging unusual $CD3^+B220^+$ population (43, 44). We did see a trend toward a higher percentage of $CD19^+$ cells in splenic lymphocytes of mice injected with mAb 3d-8b, although it was not statistically significant.

Reversal in CR1/CR2 downregulation on B cells in mice treated with mAb 3d-8b

Altered levels of CR2 expression on B cells from patients with SLE and lower levels of CR2/CR1 expression on B cells from MRL/*lpr* mice are a hallmark of B cell changes in lupus (45–47). When we stained splenic B cells for the level of CR2/CR1 using mAb 4B2 (37) (Fig. 9A) or for the level of CR1 using anti-CR1–specific mAb 8C12 (46) (Fig. 9B), we found that the reduction in CR2/CR1 level seen in older MRL/*lpr* mice was reversed by mAb 3d-8b injection to the level seen in younger MRL/*lpr* mice.

Discussion

We have found that mAb 3d-8b, which binds to the complement C3 breakdown proteins iC3b and C3d, blocks the in vivo B cell Ab responses to SRBC, a T-dependent Ag. It also abrogates the enhanced Ca^{2+} influx induced in vitro with anti-IgM/C3d complexes by blocking C3d binding to CR2. Both B cell and follicular dendritic cell interactions with C3d-bound Ags are major factors underlying proper GC formation and high-affinity Ab production as well as Ab class switching (48, 49). Consistent with an interruption of those processes, we found that mAb 3d-8b reduces GC formation and thus negatively affects primary B cell activation as well as the maturation and class switching of Ag-specific IgG. In addition, mAb 3d-8b impaired plasmablast, plasma cell, and long-term memory B cell formation. To confirm that mAb 3d-8b binds specifically to complement C3 breakdown products in vivo, we injected the mAb into C3-deficient and C3-sufficient mice and determined the kinetics of elimination from blood. The 3d-8b mAb was relatively quickly removed from the circulation in C3-sufficient mice but exhibited a longer $t_{1/2}$ in C3-deficient animals.

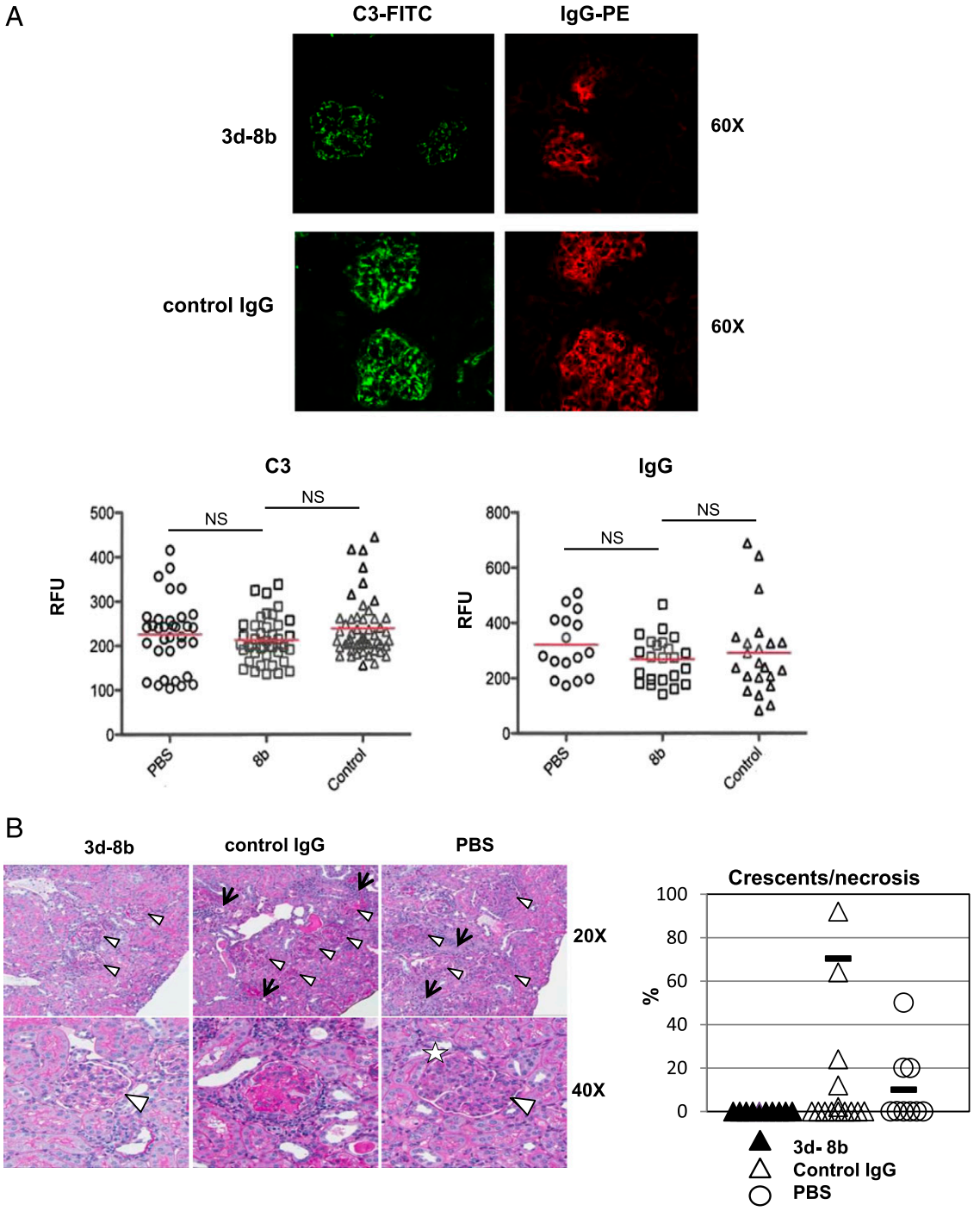

FIGURE 6. Results of assessment of C3 and IgG deposition and glomerular damage in kidneys. (**A**) Snap-frozen kidneys were sectioned, and slides were stained with anti-C3–FITC and anti-mIgGγ−PE Ab to determine the level of deposition of C3 and IgG. Representative pictures from kidney of mice injected with isotype control and mAb 3d-8b are shown. Graphs depict 50 glomeruli from kidneys of two mice injected with PBS (circles), 3d-8b (squares) and control Ab (triangles) analyzed for the level of fluorescence intensity for C3 and IgG. (**B**) Formaldehyde-fixed kidneys from mice were assayed for glomerular damage using paraffin-embedded, PAS-stained sections. Representative photos show endocapillary hypercellularity, glomeruli are indicated with arrowheads and areas of tubulointerstitial inflammation are marked with arrows. Sclerotic glomerulus with crescent formation and collagen type IV deposition is marked with a star. Increase of the number of tuft cells occluding the glomerular capillaries. The percentage of crescent/necrotic glomeruli per 50 glomeruli from each kidney is presented in the graph at right. Statistical analyses were performed by one-way ANOVA. ns, not statistically significant.

MRL/*lpr* mice spontaneously develop an autoimmune syndrome similar to human SLE, including autoantibody production and glomerulonephritis (34, 50). To study the effects of mAb 3d-8b on the development of lupus-like autoimmunity, we treated MRL/*lpr* mice with a single dose of Ab at 13–14 wk of age, early in the course of disease. In initial experiments we found that mAb 3d-8b injection decreased the level of anti-dsDNA Ab in plasma. The reduction in anti-dsDNA Ab levels was associated with a reduced level of albuminuria. In follow-up experiments, a single injection of mAb 3d-8b led to some degree of reduction of albuminuria and BUN for 8 wk after injection. The Ab is not present in the mouse body at week 8; however, the effect of the Ab injection

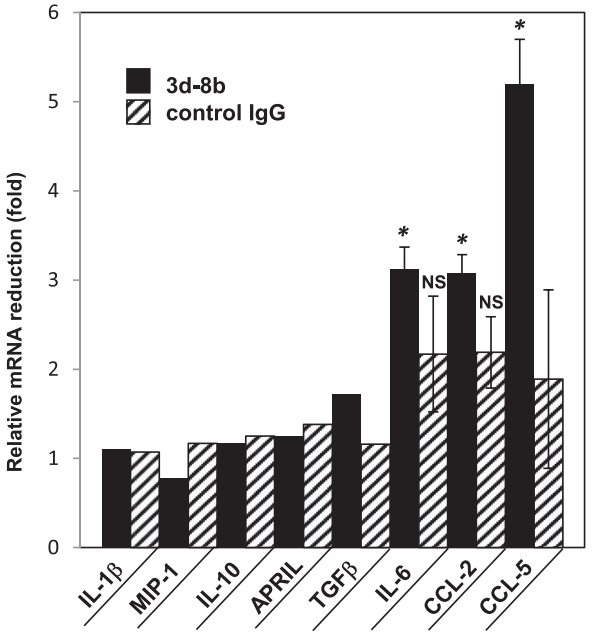

FIGURE 7. Kidney mRNA level reduction in mice treated with 3d-8b. qPCR for the chemokines in kidneys of 22-wk-old mice described in Fig. 6 and injected at week 14 with PBS, control, and mAb 3d-8b. The bars represent (average) reduction of total RNA abundance for mAb 3d-8b–injected mice (black bar) and control Ab–injected mice (stripped bar) as compared with the mice injected with PBS only. The average ΔCq for each mouse sample for a particular gene, either mAb 3d-8b– or control mAb–injected, was divided by the ΔCq average for PBS-injected mice. Statistical analyses were performed by one-way ANOVA. For statistical analysis, ΔCq for each mouse sample from mAb 3d-8b– or control Ab–injected mice was compared with ΔCq of mice from PBS-injected group. $*p < 0.05$. NS, not statistically significant.

lasts as long as 8 wk. There are some possibilities as to why the Ab has this long-lasting effect. The mAb 3d-8b injection might change B cell responsiveness following injection so that they do not produce autoantibody and do not release T cell activating factors. A second possibility is that the mAb 3d-8b–coated ICs were not able to activate newly generated B cells properly, as CR1/CR2 receptors were not able to interact with their ligands and provide a costimulatory signal to B cells. Support for the latter mechanism is provided by the observation that CR1/CR2 is not downregulated on B cells in mAb 3d-8b–injected mice. A third possibility is that mAb 3d-8b is retained on Ag complexes in B cell follicles for sufficiently prolonged periods of time to block interactions with newly developing Ag-specific B cells. These possibilities will be addressed in future experiments. Notably, the level of circulated IC was not different for the three groups of mice, whereas the level of total blood IgGγ was higher in mice injected with mAb 3d-8b. The mechanism underlying the latter finding is unknown; however, it is a striking finding in concert with the decrease in anti-dsDNA IgG autoantibody levels seen in parallel, and strongly suggests that Ag-specific autoimmune responses are particularly dependent upon the engagement of C3d-bearing autoantigens with the CR2/CD19 complex.

Glomerular C3 and IgG deposition in MRL/*lpr* kidneys increases as the disease progresses (51–53). C3 deposition in the glomeruli of mAb 3d-8b–injected mice trended toward a reduction compared with control mice, suggesting that there was less IC-mediated inflammation in the treated mice. At the end of the experiment, crescents and necrosis were not seen in the glomeruli of mice injected with mAb 3d-8b, supporting the protective effects of CR2 blockade, although this finding did not reach statistical significance.

To further understand the effects of mAb 3d-8b treatment on the earlier evolution of renal disease, it will be necessary to sacrifice treated and control mice serially through the earlier stages of disease.

The analysis of proinflammatory mRNA species by qPCR also provided evidence of decreased inflammation in the kidneys from the mAb 3d-8b–injected group. We found a very substantial reduction in expression of IL-6, a highly proinflammatory cytokine. In contrast, we did not see upregulation of anti-inflammatory IL-10 cytokine, but it has also been noted that B cell–derived IL-10 does not regulate renal pathology in MRL/*lpr* mice (54). The proinflammatory chemokine MCP-1 (MCP-1/CCL2) and CCL5 (RANTES) mRNA levels were also reduced in mAb 3d-8b–injected mice. Both chemokines recruit leukocytes into sites of inflammation; for instance, CCL2 recruits monocytes, memory T cells, and dendritic cells, whereas CCL5 is chemotactic for T cells, eosinophils, and basophils. Reduction of mRNA levels for these proinflammatory chemokines is consistent with lower inflammation and decreased renal injury in mAb 3d-8b–injected mice as well as the finding that the level of proteinuria in these mice was lower. The levels of mRNA for IL-1β, TGF-β, APRIL, and MIP-1 did not differ significantly from the levels expressed in PBS-treated mice. For the chemokines TGF-β and APRIL, we detected trends in reduction; however, the differences were not statistically significant when compared with the levels seen in PBS-injected control mice.

Flow cytometric analyses also provided important insights. Disease onset in MRL/*lpr* mice is associated not only with the well-known unusual population of $CD3^+$ $B220^+$ cells but also an upregulated level of splenic $CD19^+CD23^-CD24^-$ cells. This cell subpopulation is considered to be the splenic MZ cell subpopulation. It is not clear whether these cells are true MZ cells with all characteristics of such cells or whether these $CD23^-CD24^-$ cells are follicular B cells that have lost the CD23 marker. Staining of additional cell surface markers is needed to analyze this population. We also noted that mAb 3d-8b injection was associated with downregulation of the mature cell subpopulation ($CD23^+CD24^-$) in older mice, although these changes were not statistically significant. When PBS or control mAb was injected into 7- or 14-wk-old mice, we did not see any significant changes in these B cell subpopulations in the spleen after either 24 h or 1 wk, confirming that high-dose Ab injection does not affect the proportion of splenic cells subpopulations. We also did not see any effects of mAb 3d-8b on the $CD3^+B220^+$ subpopulation (data not shown). Likewise, we did not see any changes in either $CD8^+$ or $CD4^+$ T cells. These data point to the fact that injection of high-dose mAb 3d-8b does not induce elimination of any studied cell population or B cell subpopulation. Some trend in $CD19^+$ cell upregulation was observed in older mice injected with mAb 3d-8b compared with mice that were given control Ab or PBS injections. No similar $CD19^+$ cell upregulation was observed for young mice. In contrast, a striking observation was made when we analyzed splenic B cells for the levels of CR2/CR1 or CR1 alone expression. We found that injection of mAb 3d-8b reversed the CR2/CR1 downregulation associated with lupus disease development. Altered levels of CR2 expression on B cells from patients with SLE and lower levels of CR2/CR1 expression on B cells from MRL/*lpr* mice are a hallmark of SLE (45–47). Engagement of CR2 with Ag complexes induces CR2 shedding or internalization (55, 56). However, lupus patients, as well as other autoimmune disorder patients, have

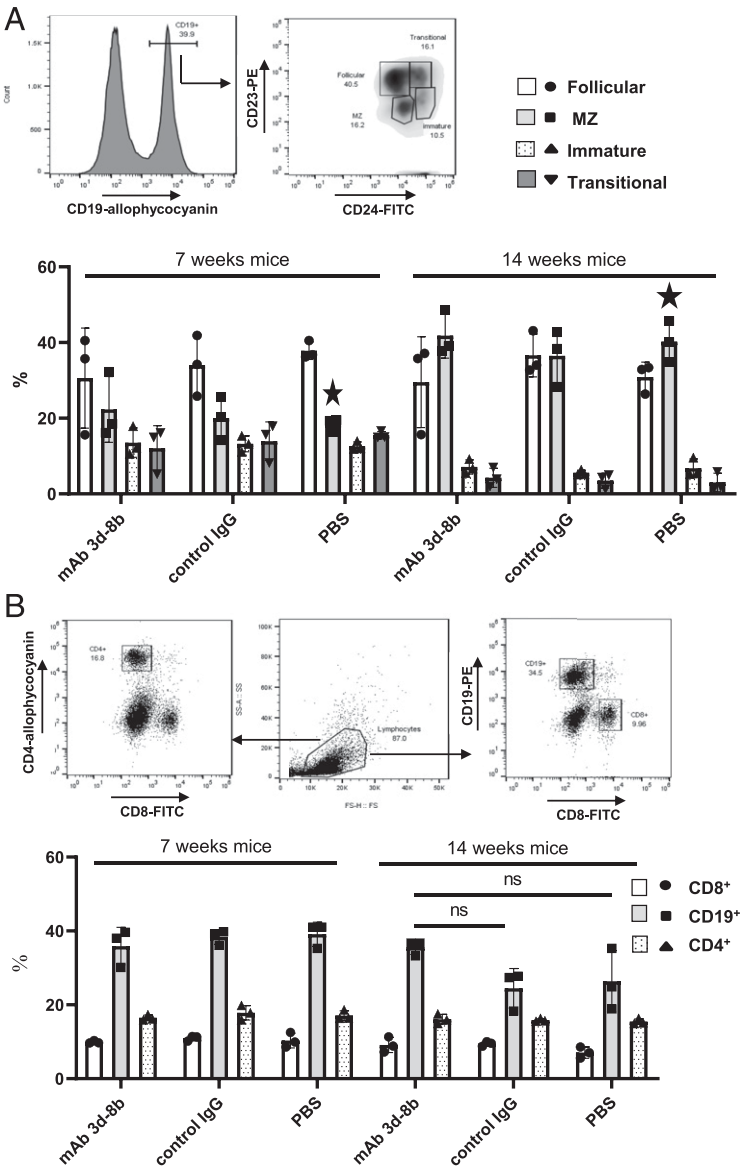

FIGURE 8. Effect of 3d-8b mAb injection on splenic B cell subpopulations in addition to T and B cell populations in spleen. (**A**) Seven- and fourteen-week-old MRL/*lpr* mice (three per group) were injected with 2 mg/mouse of mAb 3d-8b, isotype control, or PBS alone. One week later, spleens were taken, and cells were stained with CD19–allophycocyanin, CD23–PE, or CD24–FITC. Histogram represents gating strategy for $CD19^+$ cells. $CD19^+$ cells were analyzed for levels of expression for CD24 and CD23 markers. Percentage of follicular ($CD23^+$, $CD24^{lo}$), MZ ($CD23^-$, $CD24^{lo}$), transitional ($CD23^+$, $CD24^{hi}$), and immature ($CD23^-$,$CD24^{hi}$) cells on gated $CD19^+$ cells was calculated. Bars represent mean percentage data calculated for each mouse in particular group. Stars show the differences in MZ cells between young and old MRL/*lpr* mice. Error bars represent SD for a particular group of data. (**B**) Splenic cells from mice described in (A) were stained with anti-CD4–allophycocyanin, anti-CD8–FITC and anti-CD19–PE Ab. The average percentage of CD8, CD4, and CD19-positive spleen cells in total cell population is presented in the bar graph. Error bars represent SD for a particular group of data. Statistical analyses were performed by one-way ANOVA, comparing data obtained for mAb 3d-8b–injected mice to control Ab– or PBS-injected mice. ns, not statistically significant.

reduced levels of soluble CR2 (57), arguing against excessive shedding but pointing, rather, to internalization, which occurs when IC decorated by C3d activate B cells through BCR (IgM) and CR2. It is possible that 3d-8b mAb blocks CR1 from being ligated with iC3b and CR2 from C3d ligation, and thus prevents B cells from robust activation through BCR signals supplemented with CR2 signal costimulation. Treatment may also prevent CR1 from being internalized or shed and thus allows CR1 to perform its function of maintaining tolerance.

There remains a possibility that FcγR (I–III), expressed on macrophages, could bind to the Fc portion of the mAb 3d-8b when it is bound to IC decorated by iC3b/C3d and thus remove IC through the liver and spleen. However, we did not see reduction in IC in plasma of mice injected with mAb 3d-8b. It is also possible that IC bound by mAb 3d-8b may exhibit reduced clearance because of their inability to bind to complement receptors expressed on mouse platelets and thus be removed efficiently through the liver or spleen. If this is true, the same mechanism can prevent IC from being bound to tissues, such as kidney glomeruli, and thus prevent glomeruli from injury caused by IC deposition.

FcγRII on B cells could be involved in the similar binding of the Fc tail of mAb 3d-8b and generate an inhibitory B cell signal. Despite those possibilities, the most parsimonious conclusion is that mAb 3d-8b–covered IC prevent CR1/CR2 from coupling to its ligands and thus decrease or abrogate the CR2/C3d costimulatory signal. As we clearly see that B cells from mAb 3d-8b–injected mice do not show CR1/CR2 downregulation associated with B cell activation in lupus and other autoimmune diseases. The prevention of CR1 and CR2 levels from downregulation is the major mechanism playing a role in decreasing autoantibody production and, possibly, reducing proteinuria and renal injury in MRL/*lpr* mice. In addition, this conclusion is supported by previously published data (11, 32) showing that soluble CR2(SCR 1-4) alone, without an Fc domain, was capable of modestly reducing anti-dsDNA Ab levels and renal injury, again suggesting that blocking the CR2/C3d–dependent BCR costimulatory signal has a generally beneficiary effect on disease burden in this lupus-prone mouse strain.

In summary, we show that C3d-bound Ag interactions with CR2 promote the induction of autoimmunity and lead to high-affinity IgG class-switched autoantibody production to self-antigens. Whether this process is important in the first steps of molecular mimicry to foreign Ags or to internal immune responses that can lead to autoantibody production are topics for future research. Nevertheless,

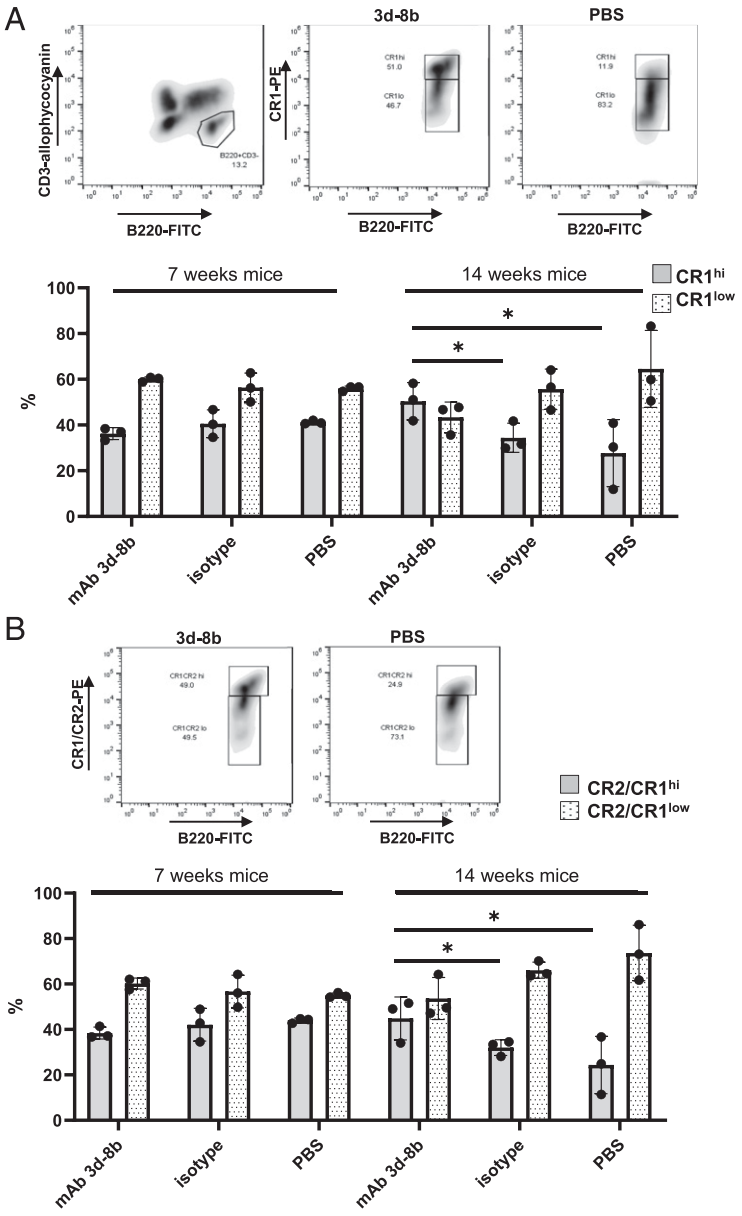

FIGURE 9. Injection of mAb 3d-8b prevents disease-associated downregulation of CR2/CR1. Seven- and fourteen-week-old mice (three per group) were injected with mAb 3d-8b, control Ab, or PBS. One week later, splenocytes isolated from each individual spleen were stained with CD3–allophycocyanin, B220–FITC and anti-CR1–PE (mAb 8C12) in (**A**) or CD3–allophycocyanin, B220–FITC and anti-CR2/CR1–PE (mAb 4B2) in (**B**). Gated $B220^{+}CD3^{-}$ splenocytes (B cells) were analyzed for the levels of CR1 or CR1/CR2 proteins. For that, the $B220^{+}CD3^{-}$ cell gate was opened for B220–FITC and anti-CR1–PE in (A) or anti-CR1/CR2–PE in (B), and cells were gated for CR1 or CR1/CR2 high (hi; upper box) and low (lo; lower box) based on CR1 or CR1/CR2 levels seen in young MRL/*lpr* mouse (7 wk). As an example, we have two representative plots, one showing hi and lo subpopulations in mAb 3d-8b–injected group and the other showing the same populations in PBS-injected older mice (14 wk). The bars (mean ± SD) represent percentage of the hi and lo cells in $B220^{+}$ population accordantly to the injections mice received. To perform statistical analyses, the data for cells designated as the hi population from mAb 3d-8b–injected mice were compared with either data of hi population in control Ab–injected group or to the data for the hi population in PBS-injected group. Statistical analyses were performed by one-way ANOVA. $*p < 0.05$.

we show in this study that the disruption of the CR2 costimulation signal by blocking C3d binding to the receptor can be an effective treatment strategy.

Acknowledgments

We thank University of Colorado veterinary technicians Matt Palmer, Scott Sand, and Laura Richardson for assistance.

Disclosures

V.M.H., J.M.T., and L.K. are inventors on patents related to this work. V.M.H. and J.M.T. receive royalties from Alexion Pharmaceuticals, Inc., and are consultants for AdMIRx, Inc., a company developing complement inhibitors. J.M.T. and L.K. will receive royalty income from AdMIRx. The other authors have no financial conflicts of interest.

References

1. Tsokos, G. C. 2011. Systemic lupus erythematosus. *N. Engl. J. Med.* 365: 2110–2121.
2. Davidson, A. 2016. What is damaging the kidney in lupus nephritis? *Nat. Rev. Rheumatol.* 12: 143–153.
3. Liu, Z., and A. Davidson. 2012. Taming lupus-a new understanding of pathogenesis is leading to clinical advances. *Nat. Med.* 18: 871–882.
4. Kamal, A., and M. Khamashta. 2014. The efficacy of novel B cell biologics as the future of SLE treatment: a review. *Autoimmun. Rev.* 13: 1094–1101.
5. van Vollenhoven, R. F., I. Parodis, and A. Levitsky. 2013. Biologics in SLE: towards new approaches. *Best Pract. Res. Clin. Rheumatol.* 27: 341–349.
6. Carroll, M. C. 1998. The lupus paradox. *Nat. Genet.* 19: 3–4.
7. Bao, L., I. Osawe, M. Haas, and R. J. Quigg. 2005. Signaling through up-regulated C3a receptor is key to the development of experimental lupus nephritis. *J. Immunol.* 175: 1947–1955.
8. Bao, L., I. Osawe, T. Puri, J. D. Lambris, M. Haas, and R. J. Quigg. 2005. C5a promotes development of experimental lupus nephritis which can be blocked with a specific receptor antagonist. *Eur. J. Immunol.* 35: 2496–2506.
9. Bao, L., and R. J. Quigg. 2007. Complement in lupus nephritis: the good, the bad, and the unknown. *Semin. Nephrol.* 27: 69–80.
10. Merle, N. S., R. Noe, L. Halbwachs-Mecarelli, V. Fremeaux-Bacchi, and L. T. Roumenina. 2015. Complement system part II: role in immunity. *Front. Immunol.* 6: 257.
11. Sekine, H., P. Ruiz, G. S. Gilkeson, and S. Tomlinson. 2011. The dual role of complement in the progression of renal disease in NZB/W F(1) mice and alternative pathway inhibition. *Mol. Immunol.* 49: 317–323.
12. Botto, M., and M. J. Walport. 2002. C1q, autoimmunity and apoptosis. *Immunobiology* 205: 395–406.
13. Manderson, A. P., M. Botto, and M. J. Walport. 2004. The role of complement in the development of systemic lupus erythematosus. *Annu. Rev. Immunol.* 22: 431–456.
14. Mitchell, D. A., P. R. Taylor, H. T. Cook, J. Moss, A. E. Bygrave, M. J. Walport, and M. Botto. 1999. Cutting edge: C1q protects against the development of glomerulonephritis independently of C3 activation. *J. Immunol.* 162: 5676–5679.

15. Einav, S., O. O. Pozdnyakova, M. Ma, and M. C. Carroll. 2002. Complement C4 is protective for lupus disease independent of C3. *J. Immunol.* 168: 1036–1041.
16. Elliott, M. K., T. Jarmi, P. Ruiz, Y. Xu, V. M. Holers, and G. S. Gilkeson. 2004. Effects of complement factor D deficiency on the renal disease of MRL/lpr mice. *Kidney Int.* 65: 129–138.
17. Watanabe, H., G. Garnier, A. Circolo, R. A. Wetsel, P. Ruiz, V. M. Holers, S. A. Boackle, H. R. Colten, and G. S. Gilkeson. 2000. Modulation of renal disease in MRL/lpr mice genetically deficient in the alternative complement pathway factor B. *J. Immunol.* 164: 786–794.
18. Ahearn, J. M., and D. T. Fearon. 1989. Structure and function of the complement receptors, CR1 (CD35) and CR2 (CD21). *Adv. Immunol.* 46: 183–219.
19. Ames, R. S., Y. Li, H. M. Sarau, P. Nuthulaganti, J. J. Foley, C. Ellis, Z. Zeng, K. Su, A. J. Jurewicz, R. P. Hertzberg, et al. 1996. Molecular cloning and characterization of the human anaphylatoxin C3a receptor. *J. Biol. Chem.* 271: 20231–20234.
20. Bradbury, L. E., V. S. Goldmacher, and T. F. Tedder. 1993. The CD19 signal transduction complex of B lymphocytes. Deletion of the CD19 cytoplasmic domain alters signal transduction but not complex formation with TAPA-1 and Leu 13. *J. Immunol.* 151: 2915–2927.
21. Verschoor, A., M. A. Brockman, D. M. Knipe, and M. C. Carroll. 2001. Cutting edge: myeloid complement C3 enhances the humoral response to peripheral viral infection. *J. Immunol.* 167: 2446–2451.
22. Sekine, H., C. M. Reilly, I. D. Molano, G. Garnier, A. Circolo, P. Ruiz, V. M. Holers, S. A. Boackle, and G. S. Gilkeson. 2001. Complement component C3 is not required for full expression of immune complex glomerulonephritis in MRL/lpr mice. *J. Immunol.* 166: 6444–6451.
23. Machida, T., N. Sakamoto, Y. Ishida, M. Takahashi, T. Fujita, and H. Sekine. 2018. Essential roles for mannose-binding lectin-associated serine protease-1/3 in the development of lupus-like glomerulonephritis in MRL/*lpr* mice. *Front. Immunol.* 9: 1191.
24. Sahu, A., S. N. Isaacs, A. M. Soulika, and J. D. Lambris. 1998. Interaction of vaccinia virus complement control protein with human complement proteins: factor I-mediated degradation of C3b to iC3b1 inactivates the alternative complement pathway. *J. Immunol.* 160: 5596–5604.
25. Ahearn, J. M., M. B. Fischer, D. Croix, S. Goerg, M. Ma, J. Xia, X. Zhou, R. G. Howard, T. L. Rothstein, and M. C. Carroll. 1996. Disruption of the Cr2 locus results in a reduction in B-1a cells and in an impaired B cell response to T-dependent antigen. *Immunity* 4: 251–262.
26. Donius, L. R., J. M. Handy, J. J. Weis, and J. H. Weis. 2013. Optimal germinal center B cell activation and T-dependent antibody responses require expression of the mouse complement receptor Cr1. *J. Immunol.* 191: 434–447.
27. Molina, H., V. M. Holers, B. Li, Y. Fung, S. Mariathasan, J. Goellner, J. Strauss-Schoenberger, R. W. Karr, and D. D. Chaplin. 1996. Markedly impaired humoral immune response in mice deficient in complement receptors 1 and 2. *Proc. Natl. Acad. Sci. USA* 93: 3357–3361.
28. Wu, X., N. Jiang, Y. F. Fang, C. Xu, D. Mao, J. Singh, Y. X. Fu, and H. Molina. 2000. Impaired affinity maturation in $Cr2^{-/-}$ mice is rescued by adjuvants without improvement in germinal center development. *J. Immunol.* 165: 3119–3127.
29. Rosain, J., C. Miot, N. Lambert, M. C. Rousselet, I. Pellier, and C. Picard. 2017. CD21 deficiency in 2 siblings with recurrent respiratory infections and hypogammaglobulinemia. *J. Allergy Clin. Immunol. Pract.* 5: 1765–1767.e3
30. Wu, X., N. Jiang, C. Deppong, J. Singh, G. Dolecki, D. Mao, L. Morel, and H. D. Molina. 2002. A role for the Cr2 gene in modifying autoantibody production in systemic lupus erythematosus. *J. Immunol.* 169: 1587–1592.
31. Das, A., B. A. Heesters, A. Bialas, J. O'Flynn, I. R. Rifkin, J. Ochando, N. Mittereder, G. Carlesso, R. Herbst, and M. C. Carroll. 2017. Follicular dendritic cell activation by TLR ligands promotes autoreactive B cell responses. *Immunity* 46: 106–119.
32. Sekine, H., T. T. Kinser, F. Qiao, E. Martinez, E. Paulling, P. Ruiz, G. S. Gilkeson, and S. Tomlinson. 2011. The benefit of targeted and selective inhibition of the alternative complement pathway for modulating autoimmunity and renal disease in MRL/lpr mice. *Arthritis Rheum.* 63: 1076–1085.
33. Cohen, P. L., and R. A. Eisenberg. 1992. The lpr and gld genes in systemic autoimmunity: life and death in the Fas lane. [Published erratum appears in 1993 *Immunol. Today* 14: 97.] *Immunol. Today* 13: 427–428.
34. Perry, D., A. Sang, Y. Yin, Y. Y. Zheng, and L. Morel. 2011. Murine models of systemic lupus erythematosus. *J. Biomed. Biotechnol.* 2011: 271694.
35. Thurman, J. M., L. Kulik, H. Orth, M. Wong, B. Renner, S. A. Sargsyan, L. M. Mitchell, D. E. Hourcade, J. P. Hannan, J. M. Kovacs, et al. 2013. Detection of complement activation using monoclonal antibodies against C3d. *J. Clin. Invest.* 123: 2218–2230.
36. Heyman, B., G. Holmquist, P. Borwell, and U. Heyman. 1984. An enzyme-linked immunosorbent assay for measuring anti-sheep erythrocyte antibodies. *J. Immunol. Methods* 68: 193–204.
37. Kulik, L., F. B. Hewitt, V. C. Willis, R. Rodriguez, S. Tomlinson, and V. M. Holers. 2015. A new mouse anti-mouse complement receptor type 2 and 1 (CR2/CR1) monoclonal antibody as a tool to study receptor involvement in chronic models of immune responses and disease. *Mol. Immunol.* 63: 479–488.
38. Kulik, L., K. J. Marchbank, T. Lyubchenko, K. A. Kuhn, G. A. Liubchenko, C. Haluszczak, M. G. Gipson, S. A. Boackle, and V. M. Holers. 2007. Intrinsic B cell hypo-responsiveness in mice prematurely expressing human CR2/CD21 during B cell development. [Published erratum appears in 2007 *Eur. J. Immunol.* 37: 1149.] *Eur. J. Immunol.* 37: 623–633.
39. Pisetsky, D. S., and D. V. Peters. 1981. A simple enzyme-linked immunosorbent assay for antibodies to native DNA. *J. Immunol. Methods* 41: 187–200.
40. Carlsson, F., A. Getahun, C. Rutemark, and B. Heyman. 2009. Impaired antibody responses but normal proliferation of specific CD4+ T cells in mice lacking complement receptors 1 and 2. *Scand. J. Immunol.* 70: 77–84.
41. Henson, S. E., D. Smith, S. A. Boackle, V. M. Holers, and D. R. Karp. 2001. Generation of recombinant human C3dg tetramers for the analysis of CD21 binding and function. *J. Immunol. Methods* 258: 97–109.
42. Wang, W., J. Rangel-Moreno, T. Owen, J. Barnard, S. Nevarez, H. T. Ichikawa, and J. H. Anolik. 2014. Long-term B cell depletion in murine lupus eliminates autoantibody-secreting cells and is associated with alterations in the kidney plasma cell niche. *J. Immunol.* 192: 3011–3020.
43. Ashman, R. F., N. Singh, and P. S. Lenert. 2017. Abnormal thymic maturation and lymphoproliferation in MRL-Fas $^{lpr/lpr}$ mice can be partially reversed by synthetic oligonucleotides: implications for systemic lupus erythematosus and autoimmune lymphoproliferative syndrome. [Published erratum appears in 2017 *Lupus* 26: 787.] *Lupus* 26: 734–745.
44. Morse, H. C., III, W. F. Davidson, R. A. Yetter, E. D. Murphy, J. B. Roths, and R. L. Coffman. 1982. Abnormalities induced by the mutant gene Ipr: expansion of a unique lymphocyte subset. *J. Immunol.* 129: 2612–2615.
45. Holers, V. M., and S. A. Boackle. 2004. Complement receptor 2 and autoimmunity. *Curr. Dir. Autoimmun.* 7: 33–48.
46. Takahashi, K., Y. Kozono, T. J. Waldschmidt, D. Berthiaume, R. J. Quigg, A. Baron, and V. M. Holers. 1997. Mouse complement receptors type 1 (CR1; CD35) and type 2 (CR2;CD21): expression on normal B cell subpopulations and decreased levels during the development of autoimmunity in MRL/lpr mice. *J. Immunol.* 159: 1557–1569.
47. Wehr, C., H. Eibel, M. Masilamani, H. Illges, M. Schlesier, H. H. Peter, and K. Warnatz. 2004. A new CD21low B cell population in the peripheral blood of patients with SLE. *Clin. Immunol.* 113: 161–171.
48. Fang, Y., C. Xu, Y. X. Fu, V. M. Holers, and H. Molina. 1998. Expression of complement receptors 1 and 2 on follicular dendritic cells is necessary for the generation of a strong antigen-specific IgG response. *J. Immunol.* 160: 5273–5279.
49. Qin, D., J. Wu, M. C. Carroll, G. F. Burton, A. K. Szakal, and J. G. Tew. 1998. Evidence for an important interaction between a complement-derived CD21 ligand on follicular dendritic cells and CD21 on B cells in the initiation of IgG responses. *J. Immunol.* 161: 4549–4554.
50. Watson, M. L., J. K. Rao, G. S. Gilkeson, P. Ruiz, E. M. Eicher, D. S. Pisetsky, A. Matsuzawa, J. M. Rochelle, and M. F. Seldin. 1992. Genetic analysis of MRL-lpr mice: relationship of the Fas apoptosis gene to disease manifestations and renal disease-modifying loci. *J. Exp. Med.* 176: 1645–1656.
51. Ault, B. H., and H. R. Colten. 1994. Cellular specificity of murine renal C3 expression in two models of inflammation. *Immunology* 81: 655–660.
52. Passwell, J., G. F. Schreiner, M. Nonaka, H. U. Beuscher, and H. R. Colten. 1988. Local extrahepatic expression of complement genes C3, factor B, C2, and C4 is increased in murine lupus nephritis. *J. Clin. Invest.* 82: 1676–1684.
53. Welch, T. R., L. S. Beischel, and D. P. Witte. 1993. Differential expression of complement C3 and C4 in the human kidney. *J. Clin. Invest.* 92: 1451–1458.
54. Teichmann, L. L., M. Kashgarian, C. T. Weaver, A. Roers, W. Müller, and M. J. Shlomchik. 2012. B cell-derived IL-10 does not regulate spontaneous systemic autoimmunity in MRL.Fas(lpr) mice. *J. Immunol.* 188: 678–685.
55. Masilamani, M., D. Kassahn, S. Mikkat, M. O. Glocker, and H. Illges. 2003. B cell activation leads to shedding of complement receptor type II (CR2/CD21). *Eur. J. Immunol.* 33: 2391–2397.
56. Tessier, J., A. Cuvillier, F. Glaudet, and A. A. Khamlichi. 2007. Internalization and molecular interactions of human CD21 receptor. *Mol. Immunol.* 44: 2415–2425.
57. Masilamani, M., R. Nowack, T. Witte, M. Schlesier, K. Warnatz, M. O. Glocker, H. H. Peter, and H. Illges. 2004. Reduction of soluble complement receptor 2/CD21 in systemic lupus erythomatosus and Sjogren's syndrome but not juvenile arthritis. *Scand. J. Immunol.* 60: 625–630.